Algorithms for Designing Pop-Up Cards

Zachary Abel* Erik D. Demaine† Martin L. Demaine† Sarah Eisenstat†
Anna Lubiw‡ André Schulz§ Diane L. Souvaine¶ Giovanni Viglietta‖
Andrew Winslow¶

Abstract

We prove that every simple polygon can be made as a (2D) pop-up card/book that opens to any desired angle between 0 and 360°. More precisely, given a simple polygon attached to the two walls of the open pop-up, our polynomial-time algorithm subdivides the polygon into a single-degree-of-freedom linkage structure, such that closing the pop-up flattens the linkage without collision. This result solves an open problem of Hara and Sugihara from 2009. We also show how to obtain a more efficient construction for the special case of orthogonal polygons, and how to make 3D orthogonal polyhedra, from pop-ups that open to 90°, 180°, 270°, or 360°.

1 Introduction

Pop-up books have been entertaining children with their surprising and playful mechanics since their mass production in the 1970s. But the history of pop-ups is much older [27], and they were originally used for scientific and historical illustrations. The earliest known example of a "movable book" is Matthew Paris's *Chronica Majora* (c. 1250), which uses turnable disks (volvelle) to represent a calendar and uses flaps to illustrate maps. A more recent scientific example is George Spratt's *Obstetric Tables* (1850), which uses flaps to illustrate procedures for delivering babies including by Caesarean section. From the same year, Dean & Sons' *Little Red Riding Hood* (1850) is the first known movable book where a flat page rises into a 3D scene, though here it was actuated by pulling a string.

The first known examples of *self-erecting* pop-ups, where the rise into 3D is actuated by opening the page, are a card promoting the Trinity Buildings in New York City (c. 1908), and S. Louis Girard's *Bookano Book* (c. 1930s). Modern pop-ups have taken these principles to new heights, often employing linkage-like mechanisms to form elaborate 3D shapes and motions; some good guides for designing pop-ups are [1, 3, 5, 20]. In recent years, pop-up books have risen to an

*MIT Department of Mathematics, 77 Massachusetts Ave., Cambridge, MA 02139, USA, zabel@math.mit.edu

†MIT Computer Science and Artificial Intelligence Laboratory, 32 Vassar St., Cambridge, MA 02139, USA, {edemaine,mdemaine,seisenst}@mit.edu

‡David R. Cheriton School of Computer Science, University of Waterloo, Waterloo, Ontario N2L 3G1, Canada, alubiw@uwaterloo.ca

§Institut für Mathematsche Logik und Grundlagenforschung, Universität Münster, andre.schulz@uni-muenster.de

¶Department of Computer Science, Tufts University, Medford, MA 02155, USA, {dls,awinslow}@cs.tufts.edu

‖Department of Computer Science, University of Pisa, Italy, vigliett@di.unipi.it

art form with such art books as Bataille's *ABC3D* [2], Carter's series of dot/spot books [4], and Pelhem's poetic pop-up book [26]. One striking form of pop-ups is *origamic architecture*, which form buildings and other geometric structures, and are usually each made from a single (cut) sheet of card stock. A few examples of the many origamic architecture books are [7, 8, 32]; see [11] for a thorough bibliography.

Our results. This paper investigates the computational geometry of pop-ups, in particular, algorithmic design of pop-ups. We achieve three main results:

1. Any 2D n-gon (extruded orthogonally into 3D) can be popped up by opening a book to a specified angle θ with $0 < \theta \leq 360°$, using a construction of complexity $O(n^2)$.
2. Any orthogonal n-gon (extruded orthogonally into 3D) can be popped up by opening a book to a specified orthogonal angle $\theta \in \{90°, 180°, 270°, 360°\}$, using a construction of complexity $\Theta(n)$.
3. Any orthogonal polyhedron can be popped up by opening a book to a specified orthogonal angle $\theta \in \{90°, 180°, 270°, 360°\}$, using a construction of complexity $O(n^3)$.

All of our constructions use rigid flat polygonal pieces to form single-degree-of-freedom linkage structures, which uniquely and deterministically unfold from the flat state to the open state, while avoiding collision.

Related work. Our first result solves an open problem of Hara and Sugihara [14], who gave an algorithmic construction for arbitrary polygons but without guarantees of collision avoidance (and indeed the construction sometimes requires collisions). An example of a popup constructed with this method is shown in Figure 1. Another result in computational geometry is by Uehara and Teramoto [31], who proved that when pop-ups have multiple ambiguous motions (including creases that can fold both mountain and valley), they are NP-hard to open or close.

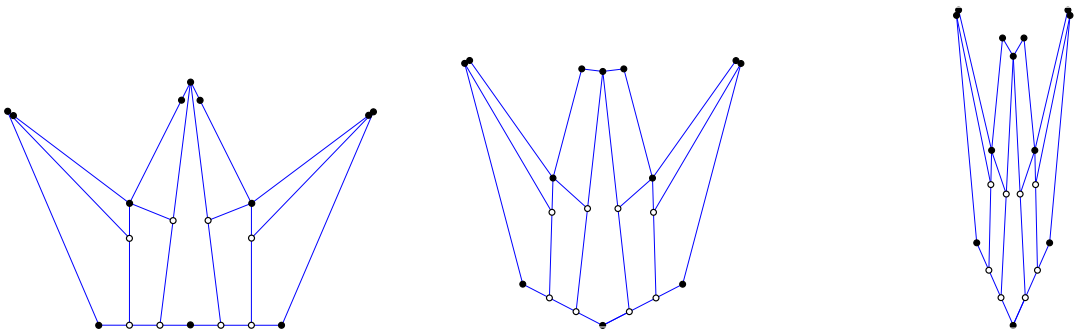

(a) (b) (c)

Figure 1: A linkage L constructed by the method of [14] in its open configuration (a) and two of its intermediate configurations (b–c). The induced linkage uses common joints (•), and flaps (○).

In computer graphics, Mitani et al. [23, 24] showed how to automatically design pop-ups within a common class of 90° origamic architecture, in which the surface is monotone (hit only once) in the view direction. This work led to Tama Software's Pop-Up Card Designer [30]. Li et al. [22]

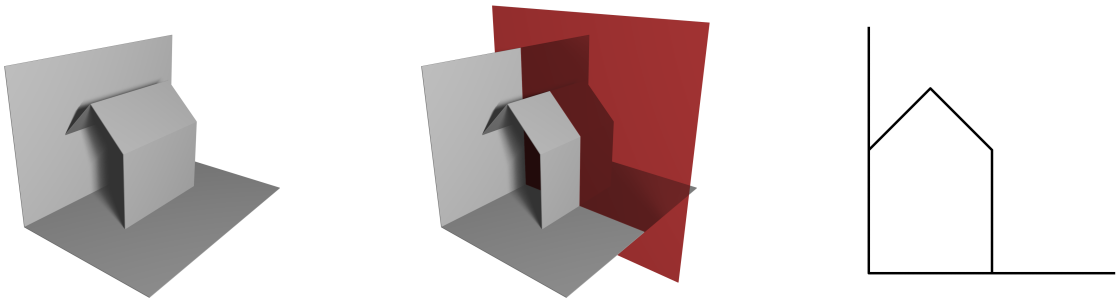

(a) The desired pop-up card. (b) Cross-section perpendicular to the spine. (c) The contents of the cross-section.

Figure 2: Three views of a desired 3D structure, before the creases and extra paper have been added to make it pop up.

developed a software system for converting a given 3D model into one that fits within this class. Several other systems enable designing and simulating pop-ups by composing standard pop-up gadgets, including Glassner's [12, 13], Popup Workshop [16, 15], Okamura and Igarashi's [25], and Iizuka et al.'s [19].

Geometric pop-ups have also been studied for specific examples of polyhedra. The first such example is a rhombic dodecahedron of the second type [10]. Other examples include the dodecahedron [29] and other Platonic solids [17, 6, 21]. These types of pop-ups are typically not attached to pages of a book, however.

Applications. Pop-ups have potential practical applications as well. Nano and micro fabrication technology are well-established for patterning 2D sheets, but remain in their infancy for 3D surfaces. Pop-ups offer a way to transform patterned 2D sheets into 3D surfaces. This idea was recently explored in the context of MEMS [18], where Hui et al. successfully manufactured a 1.8mm-tall 3D model of the UC Berkeley Campanile clock tower, with micron resolution, using pop-ups.

2 Models of Pop-Ups

Our basic model is of a book with planar front and back covers which, when opened to a desired angle θ, pops up a 3D paper construction made from pieces of stiff paper that are folded and glued to each other and to the covers. (We will not deal with the more restrictive model of origamic architecture where one piece of paper is cut and folded but not glued.)

Given a desired 3D structure, we aim to design a pop-up book that achieves it by adding creases and adding extra pieces of paper. Adding creases may be necessary in order to get the structure to fold up when the book is closed. Adding extra paper may be necessary in order to get the structure to pop up into the correct shape when the book is opened.

Until Section 5, we consider a restricted version of the problem that arises when all fold lines and all gluing lines are parallel to the spine, just as in Figure 2. In this case, a cross-section in a plane perpendicular to the spine yields a 2D pop-up: the pop-up structure and the desired shape form a planar linkage composed of rigid *bars* (line segments) connected at joints. A *joint* is a point

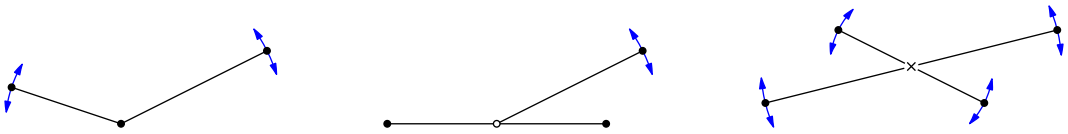

(a) A common joint. (b) A flap. (c) A sliceform.

Figure 3: The three types of joints used in this paper.

where line segments intersect, usually at an endpoint of at least one of the line segments. We distinguish three kinds of joints:

Common joints: Two or more bars are linked at one of their endpoints.

Flaps: A bar contains a joint in its interior, where an endpoint of another bar is linked. The location of the joint at the interior of the first bar is fixed.

Sliceforms: A joint (called a sliceform) can be formed by the intersection X of two bars. The intersection point X cannot shift along the bars, but the two bars can change their angle at X (scissors-like). Notice that we do not consider the two edges crossing if they are linked by a sliceform.

To distinguish the different joints in figures, we use a dot ($\bullet$) for common joints and endpoints of edges, an empty circle ($\circ$) for flaps, and a cross ($\times$) for sliceforms. Examples of the three types of joints are depicted in Figure 3.

The common joint is sufficient to simulate the other joint types. A flap can be simulated by forming a zero-area triangle among the three collinear points. A sliceform can be simulated by common joints and flaps as illustrated in Figure 4.

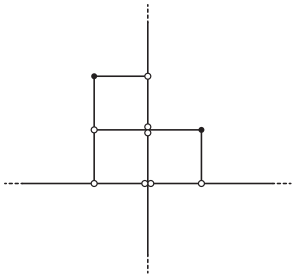

Figure 4: Simulating sliceforms.

In the 2D case, we want to construct a linkage L with one degree of freedom that folds to the desired shape, which is given by a simple polygon P. During the folding motion we require that no bars cross, and that the order of the bars emanating at a joint is preserved. Let the vertices of P be $v_1, v_2, \ldots, v_n$ labelled in counter-clockwise order. The edge incident to v_i and v_{i+1} is named e_i, the edge between v_n and v_1 is named e_n. We assume that P is contained in one of the two wedges bounded by the rays $\overrightarrow{v_1v_2}$ and $\overrightarrow{v_1v_n}$. The angle of the wedge containing P is called the *opening angle*, and the union of the rays $\overrightarrow{v_1v_2}$ and $\overrightarrow{v_1v_n}$ is called the *cover*. We require L to have the following properties:

1. In one configuration of L, the boundary of L coincides with P. We call this the *open configuration*. The linkage L contains the edges e_1 and e_n of P as bars. If a joint of L coincides with a vertex v_i in the open configuration, we name it p_i.

2. In one configuration of L that can be reached from the open configuration, all edges are collinear and p_1 is an endpoint of the union of the edges of L. This configuration is called the *closed configuration*.

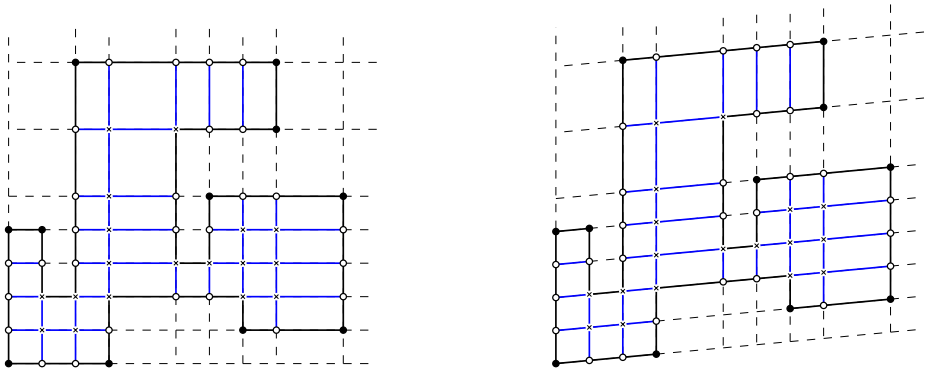

(a) (b)

Figure 5: Superimposing an orthogonal polygon. The resulting 90° pop-up for an orthogonal polygon in its open configuration (a) and in one of its intermediate configurations (b).

3. There is a unique motion that transforms the open configuration into the closed configuration. During this motion, L is contained inside the wedge defined by the cover and the opening angle decreases continuously. We refer to this motion as the *closing motion*. Every configuration of L obtained during the closing motion is called an *intermediate configuration*. The open configuration might have several joints that are opened 180°. In order to specify the folding uniquely, we prescribe for every such ambiguity the way the vertex moves during the folding motion. Collinear points in the open configuration appear naturally in pop-up structures. In the real world the folding motion at these points is prescribed by the creasing of the paper.

The *combinatorial complexity* of a 2D pop-up is equal to the number of joints in the pop-up.

3 Orthogonal Polygon Pop-Ups

In this section, we assume the polygon P is orthogonal, i.e., every edge of P is either horizontal or vertical. We show how to construct a pop-up linkage L for the polygon P with combinatorial complexity linear in n.

3.1 90° Pop-Ups

We present two ways to construct a linkage L that folds to P. An easy solution (called *superimposing*) can be constructed using sliceforms. As a first step we superimpose an orthogonal grid on P. This is done by replacing every edge of P by its supporting line. Every intersection between two lines becomes a sliceform. The linkage L is obtained by restricting this linkage to P. If one of the extended edges ends on the boundary of P then the former sliceform is replaced by a flap. Similarly, if two extended edges are joined by a sliceform that lies on a vertex of P then the sliceform is replaced by a common joint. An example of the construction is depicted in Figure 5. In order to prove that the constructed linkage has a closing motion, we define the following:

Definition 1. *A* shear *is a motion of a linkage that leaves parallel edges parallel.*

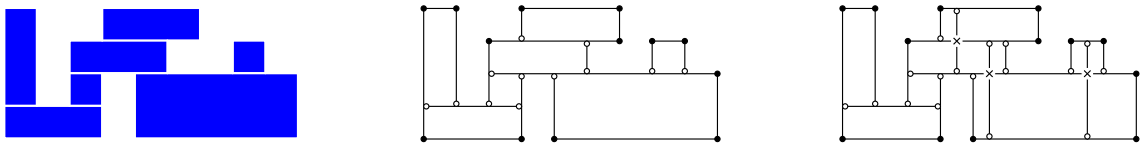

(a) (b) (c)

Figure 6: The result of h-superimposing an orthogonal polygon. (a) The induced stripes. (b) Intermediate linkage, with too many degrees of freedom. (c) Final linkage, with bracing segments to enforce a single shear motion.

We denote by a cell of a planar linkage a bounded face of its underlying graph. If the closing motion is a shear and all cells are parallelograms then no two edges can cross during the motion.

Theorem 1. *The linkage L obtained by superimposing is a pop-up fold in the sliceform model for the orthogonal polygon P with $90°$ opening angle. The combinatorial complexity of L is $O(n^2)$.*

Proof. We show that L has one degree of freedom and that the only possible motion is a shear. The proof is by induction. We define an order of the cells of the superimposed linkage: let G_k be the union of the first k cells; then G_1 must contain p_1, and for all $k \geq 1$, the interior of G_k is connected. By decreasing the opening angle, G_1 folds flat. Assume now that G_{k-1} also folds flat. The kth cell is linked with G_{k-1} by two joints which are either flaps or sliceforms. Hence adding the kth cell extends at least two edges of G_{k-1}. Because the location of these two edges is already determined by G_{k-1}, adding the kth cell does not produce any additional degree of freedom. As a consequence, the whole linkage folds with one degree of freedom, and hence the folding motion mimics the motion of the complete superimposed grid (before cutting the edges). This motion is a shear and all cells are parallelograms, which shows that L is a pop-up fold for P. Because every bar in L is an extension of an edge in P, we have $O(n)$ bars in L. To construct a joint (sliceform), two of the bars must cross, thus producing at most $O(n^2)$ joints. □

Next we show how to construct a linkage L that is a pop-up fold for P while reducing the combinatorial complexity from quadratic to linear. The process we use is called *h-superimposing*. As a first step we split P into *stripes* such that (i) each stripe is an axis aligned rectangle, and (ii) the left and right boundary edges of a stripe are a part of the boundary of P, and (iii) the union of any two stripes is not a rectangle. Such a decomposition is obtained by extending all horizontal edges of P horizontally as long as they lie in P. We say two stripes are adjacent, if they (partially) share an edge. See Figure 6(a) for an illustration.

Let L_1 be the linkage obtained by extending the horizontal edges as long as they lie within P. The newly introduced degree-3 vertices become flaps. An example of this is depicted in Figure 6(b). However, this intermediate linkage might have more than one degree of freedom. In particular, any pair of adjacent stripes that do not share a vertical bar can shear independently. To handle this, we note that for any pair of adjacent stripes, there must be at least one vertical line passing through the (strict) interior of both stripes. We call this a *bracing line* for the stripe pair. The subset of the line contained in the stripe pair is called a *bracing segment*. For each pair of adjacent stripes that do not already share a vertical bar, we add a bracing segment to the linkage, creating a sliceform joint where the segment intersects with the boundary between the stripes. See Figure 6(c) for an example. Let L_2 be the linkage resulting from the addition of the bracing segments.

Theorem 2. *The linkage L_2 obtained by* h-superimposing *defines a pop-up fold for the orthogonal polygon P with 90° opening angle. The motion of L_2 is a shear. The combinatorial complexity of L_2 is $O(n)$.*

Proof. We show that L_2 has one degree of freedom and the only possible motion is a shear. Let us fix an order of the stripes that corresponds to their first appearances in some breadth-first search traversal of the set of stripes. Let G_k be L_2 restricted to the first k stripes.

We first consider the base case. The linkage G_1 consists of a single stripe, possibly with some segments on the interior resulting from the addition of bracing segments. However, the bracing segments were added as sliceforms, so the four boundary edges of the first stripe are still bars. Because the four bars start in a rectangular configuration, the only possible motion for the bars is a shear. The additional segments on the interior of the stripe are attached to fixed locations on both horizontal edges of the stripe, so their motion is constrained to follow the same shear. Hence, the linkage G_1 has one degree of freedom, and the only motion is a shear.

Next, we consider the inductive case. When going from G_{k-1} to G_k, the change to the linkage is a local addition. Assume that in order to form G_k the kth stripe is adjacent to the ℓth stripe. Let M be the linkage L_2 restricted to stripes k and ℓ. Just as with the base case, we know that the edges of each stripe are rigid in M. Hence in any motion, stripes k and ℓ must form parallelograms. Let α be the measure of the upper-left angle of stripe k. Because stripe k must always form a parallelogram, no matter the motion, we know that the upper-left and lower-right angles must be equal to α, while the lower-left and upper-right angles must be equal to $180^\circ - \alpha$. Similarly, let β be the measure of the upper-left angle of stripe ℓ.

We wish to show that M has one degree of freedom, and that the only possible motion is a shear. Without loss of generality, assume that stripe k lies above stripe ℓ. We consider two cases:

Case A: *The kth and ℓth stripes share a vertical bar.* Without loss of generality, assume that the vertical bar lies to the right of both stripes. The horizontal bar between the two stripes must be attached to the vertical bar as a flap. Therefore, the lower-right angle of stripe k is equal to 180° minus the upper-right angle of stripe ℓ. Hence, $\alpha = 180^\circ - (180^\circ - \beta) = \beta$.

Case B: *The kth and ℓth stripes are connected by a bracing segment.* Let C_1 be the part of the kth stripe that lies to the left of the bracing segment, and let C_2 be the part of the ℓth stripe that lies to the left of the bracing segment. In the open configuration, both C_1 and C_2 are rectangles. Hence, in any motion, C_1 and C_2 must be parallelograms. Because the upper-left corner of C_1 is the upper-left corner of the kth stripe, the angle measure must be α. By similar reasoning, the measure of the upper-left corner of C_2 must be β. Hence, the measure of the lower-right corner of C_1 must be α, and the measure of the upper-right corner of C_2 must be $180^\circ - \beta$. By the properties of the sliceform, $\alpha = 180^\circ - (180^\circ - \beta) = \beta$.

As a result, we know that in either case, the stripes are constrained to move with the same shear.

By induction, the motion of G_{k-1} must be a shear with one degree of freedom. When the kth stripe is added, the restriction on M means that the combined linkage G_k has only one possible motion: a shear with one degree of freedom.

We are left with counting the vertices and edges of L_2. We begin by counting the number of stripes. The stripes are created by taking every horizontal edge of P, and extending it both left and right until it reaches some other side of the polygon. This creates at most two new horizontal bars, so the total number of bars created is $O(n)$. Each created bar forms the boundary between a

pair of adjacent stripes. Therefore, the total number of stripes is $O(n)$. The number of joints per stripe in L_1 is constant. We also add a constant number of joints (at most one sliceform and two flaps) per bracing segment. Hence, the total number of joints in L_2 is $O(n)$. Because the graph induced by L_2 is planar, the number of edges is linear in n as well. □

3.2 180°, 270°, and 360° Pop-Ups

This section is devoted to constructing pop-up folds with larger opening angle. We reduce this problem to the 90° pop-up scenario by introducing a linkage (called a *reflector gadget*) that allows us to reflect a shear. We construct the open configuration of the gadget as shown in Figure 7(a). Figure 7(b) shows an intermediate configuration.

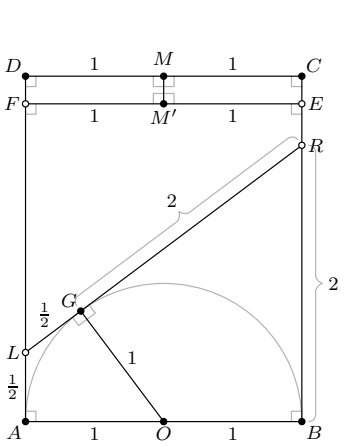

(a) The open configuration.

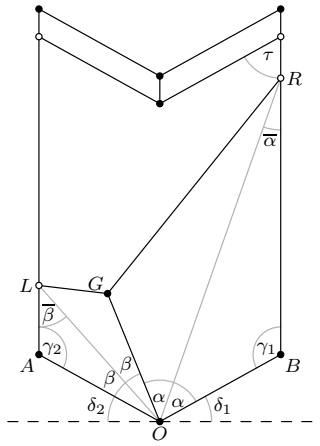

(b) An intermediate configuration.

Figure 7: The reflector gadget that helps to "reflect" two shearing motions.

Lemma 1. *The reflector gadget has one degree of freedom. Its closing motion has the following properties:*

(a) the vertical line segments in the open configuration remain vertical during the induced motion,

(b) the boundary of the gadget is symmetric with respect to a line of reflection running through $\overline{OM}$,

(c) the linkage folds to a line without introducing any crossings in an intermediate configuration.

Proof. Property (a) is ensured by the top part of the gadget. In particular, the two glued rectangles $DFMM'$ and $CEMM'$ preserve the parallelism by the induced 2 degree of freedom motion. In order to prove (b) we define a line ℓ that is orthogonal to the vertical lines of the reflector gadget and runs through O. Let δ_1 be the angle between ℓ and $\overline{OB}$ and let δ_2 be the angle between ℓ and $\overline{OA}$ (see Figure 7(b)). Notice that the angles δ_1 and δ_2 determine the shape of the boundary of the gadget.

Claim 1. *Pick δ_1 arbitrarily, such that $0 \leq \delta_1 < 90°$. Assume that the strict order of edges emanating from any vertex matches the order given by the open configuration. The configuration of the reflector is unique for $\overline{AL}$ and $\overline{BR}$ being vertical.*

Proof of Claim 1. The angle δ_1 and the vertical line through $\overline{BR}$ determine the point R, which determines in turn the point G as only point above $\overline{AB}$ with distance 1 from O and distance 2 from R. We know that A lies on a circle c_1 around O with radius 1 and that L lies on a circle c_2 around G with radius $1/2$. Let c_3 be the circle c_2 moved down by $1/2$ units vertically. Because $\overline{LA}$ is vertical and has length $1/2$, the location of A has to coincide with the intersection of c_1 and c_3. One of the intersection points is infeasible, because it coincides with G and hence does not preserve the strict order of the edges around O. The other point is therefore the only valid place for A. The location of the top part of the reflector is uniquely determined because the vertical lines are determined. □

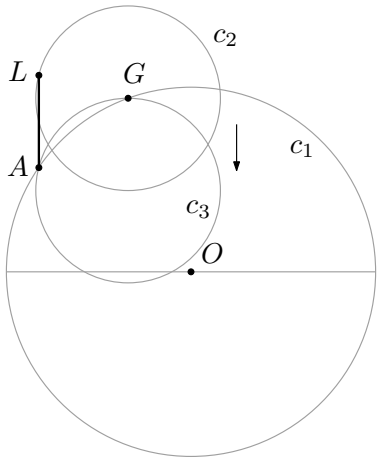

Figure 8: Construction used in the proof of Claim 1.

We show next that there is a configuration with $\delta_1 = \delta_2$, and hence this is the only solution in our setting. We define the following angles: In the triangle OBR we have the angles α (at O), γ_1 (at B), and $\bar{\alpha}$ (at R). In the triangle OAL we have the angles β (at O), γ_2 (at A), and $\bar{\beta}$ (at L). Notice that by symmetry, these angles also show up in the triangles ORG and OGL. The notation is shown in Figure 7(b). We set $\delta_1 = \delta_2$. Due to

$$\gamma_1 = 90° + \delta_1, \text{and} \quad \gamma_2 = 90° + \delta_2, \tag{1}$$

we have $\gamma_1 = \gamma_2$. As a consequence triangle OBR and triangle OLG are similar (in particular, they differ by a scaling factor of $1/2$). It follows that $\bar{\alpha} = \beta$ and $\bar{\beta} = \alpha$. In order to show that $\delta_1 = \delta_2$ gives a valid configuration we have to show that $\delta_1 + \delta_2 + 2\alpha + 2\beta = 180°$, which holds because

$$\begin{aligned}
\delta_1 + \delta_2 + 2\alpha + 2\beta &= \delta_1 + \delta_2 + \bar{\alpha} + \alpha + \bar{\beta} + \beta, \\
&= \delta_1 + \delta_2 + 180° - \gamma_1 + 180° - \gamma_2, \\
&= 180° - (\gamma_1 - \delta_1) + 180° - (\gamma_2 - \delta_2), \\
&= 90° + 90° = 180°.
\end{aligned}$$

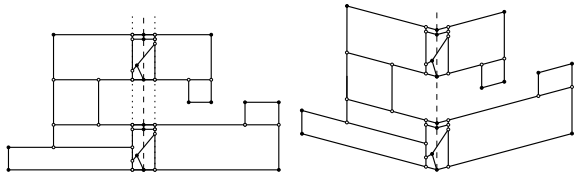

(a) (b)

Figure 9: A 180° pop-up fold constructed with the help of reflector gadgets. (a) Open configuration. (b) Some intermediate configuration.

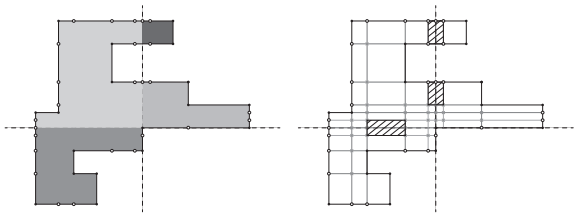

(a) (b)

Figure 10: (a) A polygon with opening angle 270°. The induced connected components are drawn with different shades of grey. (b) The pop-up linkage. The reflector gadgets have to be inserted at the crossed regions.

Property (c) follows from the fact that the order of the emanating edges around every vertex is preserved. Furthermore the vertex M' cannot cross $\overline{GR}$. To see this consider the angle τ that is realized between $\overline{EB}$ and $\overline{EM'}$. Because

$$2\bar{\alpha} = 2\beta \leq 90^\circ - \delta_2 = 90 - \delta_1 = \tau,$$

the slope at $\overline{GR}$ is larger than the slope at $\overline{EM'}$ and hence $\overline{GR}$ lies "below" $\overline{EM'}$. □

We use the properties of the reflector to combine two 90° pop-up folds to a fold with larger opening angle. We discuss 180° pop-ups first. In this case both cover edges lie on a line through p_1. To guide our construction we add a bisector s of the cover edges that runs through p_1. Furthermore, we add two parallel lines to s, such that the induced stripe contains s in the middle and no point of P except those lying on s. This stripe is called $\mathcal{S}$. The edges that "appear" when intersecting P with the boundary of $\mathcal{S}$ are added to the linkage L. We "fill" each rectangle obtained by intersecting P with $\mathcal{S}$ with a reflector gadget. The components of $P \setminus \mathcal{S}$ are turned into a linkage by h-superimposing as discussed in Section 3.1. By this, every component of $P \setminus \mathcal{S}$ supports a shearing motion. The shearing motions are linked by the reflector gadgets, so the combined linkage L has one degree of freedom. By the properties of the reflector, the left and right side of s perform a shear and both parts of P stay on their own side, relative to s. Hence it is impossible for L to self-intersect. Notice that we can always make the stripe $\mathcal{S}$ thin enough that the rectangles of $P \cap \mathcal{S}$ are not "too wide" for the reflector gadgets. See Figure 9 for an example. We conclude with:

Theorem 3. *The method described above constructs a pop-up fold for the polygon P with opening angle* 180°. *The combinatorial complexity of the linkage is $O(n)$.*

Proof. The correctness of the construction follows from the discussion above. We have at most $O(n)$ reflector gadgets, each using $O(1)$ new joints. The complexity of the remaining part is linear due to Theorem 2. □

In order to realize 270° and 360° folds we extend the 180° construction as follows. We split P into pieces by cutting it along the horizontal and vertical lines through p_1. We then turn each connected component of the split polygon into a 90° linkage, by adding bars and joints as discussed in Theorem 2. Then each piece of the polygon will be constrained to move in a shear motion,

but different pieces will not necessarily move together. To synchronize the pieces, we use reflector gadgets to connect them. To generate the space for the gadgets, we add bars that sandwich the horizontal and vertical lines through p_1, thereby creating vertical and horizontal strips in which the reflector gadgets can be placed. Because no gadgets lie inside the intersection of the vertical and horizontal strip, no two reflector gadgets interfere. Figure 10 shows an example of an 270° fold. We conclude with the following theorem:

Theorem 4. *The method described above constructs a pop-up fold for the polygon P with opening angle 270° or 360°. The combinatorial complexity of the linkage is $O(n)$.*

4 General Polygon Pop-Ups

In this section we provide a different method for constructing pop-ups of polygons. This method works for all simple P (not necessarily orthogonal), but has a higher asymptotic complexity of $O(n^2)$. Before giving the construction, we provide a key geometric lemma about the non-crossing of nested "V-fold" linkages.

4.1 Nested V-folds

We define an *outward V-fold* as the single-degree-of-freedom linkage formed by a (weakly) convex quadrilateral $ABCD$ with $AB+BC = AD+DC$. (This was called a V-fold in [14].) Such a linkage folds flat as the opening angle $\angle BAD$ decreases to zero. If, in the open configuration, the angle at C is 180° and the angle at A is less than 180° (i.e. the quadrilateral is a nontrivial triangle with C on side BD), we call this linkage a *flat outward V-fold*, and illustrate it with a small arrow as in Figure 11 in the appendix. Similarly, the linkage formed by a (weakly) non-convex quadrilateral $ABCD$ with $AB - BC = AD - DC$ has one degree of freedom and folds flat without overlap, and is called an *inward V-fold*. If the angle at C is 180° and the angle at A is less than 180° it is a *flat inward V-fold*.

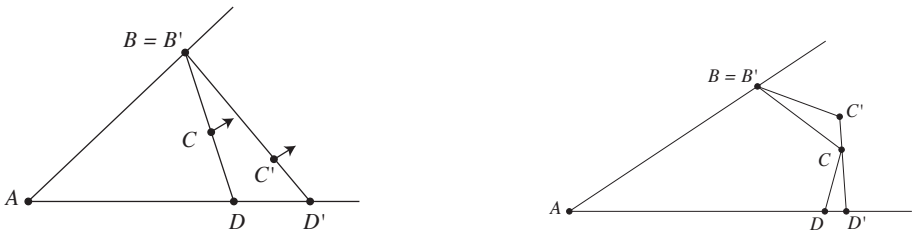

(a) Two nested outward flat V-folds

(b) A contradiction arises of we assume C hits $C'D'$

Figure 11: According to Theorem 5, flat outward V-folds $ABCD$ and $ABC'D'$ will not touch as they are folded.

Theorem 5. *(a) Let $ABCD$ and $AB'C'D'$ be flat outward V-folds on the same rays with $\triangle BAD \subset \triangle B'AD'$, where we may have $B = B'$ or $D = D'$. Then these linkages do not cross during the closing motions. In fact, they do not touch at all, except at the closing configuration and possibly at the endpoints $B = B'$ or $D = D'$ if either equality holds.*

(b) The same statement holds with "outward" replaced by "inward".

Proof. We rely on the following well-known Lemma:

Lemma 2 (Pitot's Theorem)**.** *1. A simple quadrilateral $ABCD$ (not necessarily convex) satisfies $AB + CD = AC + BD$ if and only if there is a circle internally tangent to all four side lines of the quadrilateral. By "internally tangent" we mean that the circle lies on the same side of the lines as the interior of the quadrilateral.*

2. A simple quadrilateral $ABCD$ satisfies $AB + BC = AD + DC$ if and only if either:

- *The quadrilateral is a parallelogram;*
- *$AB + AD > CB + CD$, no pair of opposite sides are parallel, and there exists a circle internally tangent to lines AB and AD and externally tangent to lines CB and CD; or*
- *$AB + AD < CB + CD$, no pair of opposite sides are parallel, and there exists a circle externally tangent to lines AB and AD and internally tangent to lines CB and CD.*

Proofs of these facts can be obtained by defining $P = AB \cap CD$ (if $AB \nparallel CD$) and comparing incircles or excircles of triangles APD and BPC.

We first prove part (a) of Theorem 5. It suffices to prove the theorem in the case that $B = B'$: indeed, if $B \neq B'$ and $D \neq D'$ then pick $C'' \in BD'$ such that $ABC''D'$ is a flat outward V-fold and apply the theorem to $ABCD \subset ABC''D'$ and $ABC''D' \subset AB'C'D'$. So we may assume $B = B'$ and $D \neq D'$.

First let us show that C never touches $C'D'$ except possibly at the closing configuration. If it did, then fix the opening angle at the first time that C lies on segment $C'D'$, as in Figure 11—this angle exists by continuity. We have $AB+BC-AD-DC = 0 = AD+DD'+D'C+CC'-AB-BC'$, and adding these expressions produces

$$0 = (BC + CC' - BC') + (DD' + D'C - DC) \geq 0 + 0,$$

so by triangle inequality both triangles $BC'C$ and CDD' must be flat. It follows that quadrilaterals $ABCD \subset ABC'D'$ have equal area and are thus equal, contradicting the assumption $D \neq D'$. So C never touches $C'D'$ until both quadrilaterals have area 0 at the closing configuration.

Now suppose that C ever lies on BC' during the closing motion. Consider the largest opening angle θ_0 for which $C \in BC'$, i.e. the first such angle reached during the closing motion. We'll show that C lies outside quadrilateral $ABC'D'$ at angle $\theta_0 + \epsilon$ for some sufficiently small ϵ, contradicting the assumed maximality of θ_0. For this, consider increasing the opening angle θ at a constant rate starting from θ_0, while holding A, D, and D' fixed. We will compute the velocities of B, C, and C' and show that C moves strictly outside $ABC'D'$ to the first order, which implies that it does so for all opening angles $\theta_0 + \epsilon$ for all sufficiently small $\epsilon > 0$. Now fix the opening angle at θ_0.

Note that $BC + CD < AB + AD$ by triangle inequality on the original configuration because $ABCD$ is a flat V-fold, and similarly $BC' + C'D' < AB + AD'$. By Lemma 2, it follows that we may define points $P = AB \cap CD$ and $P' = AB \cap C'D'$, and furthermore that there exist circles Ω and Ω' such that Ω is internally tangent to AB and AD and externally tangent to CB and CD, and likewise Ω' is internally tangent to lines AB and AD' and externally tangent to lines BC' and CD . But three of these lines coincide, so $\Omega = \Omega'$, and in particular, Ω is externally tangent to line $C'D'$. Because D is between A and D', it follows that P' is between A and P—in fact, P' is between B and P, as in Figure 12.

The velocity vector v_B of point B is perpendicular to AB, and we normalize so that $|v_B| = |BP|$. In other words, if r is the counter-clockwise rotation by 90°, we have $r(\overrightarrow{BP}) = v_B$ as vectors. Let

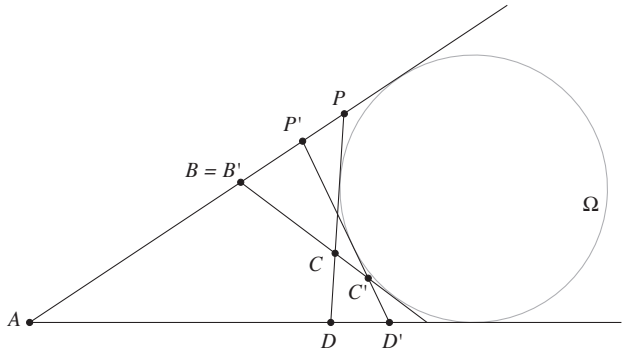

Figure 12: All five lines are tangent to a single circle by Pitot's theorem.

v_C and $v_{C'}$ be the resulting velocities of C and C'. Vector v_C satisfies $v_C \perp DC$ and $v_C - v_B \perp BC$, which uniquely determines $v_C = r(\overrightarrow{CP})$.

Pick the point Q on line BC so that $PQ \parallel C'D'$, and note that B, C', Q are collinear in that order because $BP'P$ are collinear in that order. By reasoning similar to that for v_C, we derive that $v_{C'} = r(\overrightarrow{QP})$.

So the angular velocity of C rotating clockwise around B (as in Figure 12) is equal to $|BC|/|BC| = 1$, and similarly the angular velocity of C' around B is $|BQ|/|BC'| > 1$. So C moves out of quadrilateral $ABCD$ to the first order, which completes the proof.

If $ABCD \subset AB'C'D'$ begin as flat *inward* V-folds, then we may assume $B = B'$ as above, and Lemma 2 guarantees that quadrilaterals $ABCD$ and $ABC'D'$ have a common *inscribed* circle (i.e. tangent to all lines internally). The rest of the proof proceeds as above. □

4.2 The General Pop-Up Construction: The Method

We are now able to describe the construction for pop-ups of general polygons. As in Section 2, we wish to construct a one-degree-of-freedom linkage L contained in simple polygon $P = v_1 v_2 \cdots v_n$, where P is contained in the wedge formed by rays $v_1 v_2$ and $v_1 v_n$. We sometimes refer to the crease point v_1 as O. The opening angle θ of the original configuration, namely the angle of polygon P at vertex O, is not constrained to $\{90°, 180°, 270°, 360°\}$ in this section: it may take any value $0 < \theta \leq 360°$.

First we discuss the general strategy and provide a linkage L_1 that has a pop-up motion for polygon P but has more than one degree of freedom. Later we brace the linkage to remove the excess flexibility.

We first subdivide the wedge around O containing P by rays starting at O, where there is one such ray through each vertex of P and additional rays are inserted so that consecutive rays form acute angles. Suppose $r_1, \ldots, r_t$ are these rays in order around $O = v_1$, starting at $r_1 = \overrightarrow{Ov_2}$ and ending at $r_t = \overrightarrow{Ov_n}$. The region of the plane between rays r_i and r_{i+1} is the *ith wedge*, W_i. We subdivide polygon P by these rays: any positive length segment of a ray r_i contained in P or its boundary is inserted as a single bar in linkage L_1 and is called a *wall segment*. Notice that edges of P may be wall segments. Also, by slight abuse of terminology, a positive length subsegment of a wall segment is also called a wall segment. Any isolated points on $r_i \cap P$ are necessarily vertices of P and are called *wall points*.

The rays r_i—or equivalently the wall segments—subdivide P into a number of triangles and quadrilaterals, called *cells*. Each cell has two wall portions on consecutive rays: at least one of these is a wall segment, and the other may be a wall segment or point. A cell that has two wall segments is called an *internal cell*, and those with a wall point are *ear cells*. Two cells are *adjacent* if they share a wall segment. By adding at most one new ray for each ear cell, (and renumbering the rays as necessary), we may assume that each ear cell is adjacent to a unique interior cell.

The rays r_i also subdivide the boundary of P into segments. On each such segment AB that is not a wall segment (which implies A and B are on consecutive rays), insert a joint C at the point that would make $OACB$ an outward V-fold at O, i.e., C is the unique point on AB with $OA + AC = OB + BC$. This linkage L_1 serves our first stated purpose:

Lemma 3. *The linkage L_1, constructed from P by adding wall segments and extra boundary vertices as described here, can be continuously folded flat without overlap.*

Proof. Let ϕ_i be the angle of wedge W_i, i.e., the angle between rays r_i and r_{i+1} at O. Consider any continuous rotation of rays $r_1, \ldots, r_t$ around O so that all angles $\phi_1, \ldots, \phi_{t-1}$ decrease monotonically to 0. Let each wall portion on ray r_i rotate around O to stay on ray r_i, and for each boundary portion ACB of P within wedge W_i, let ACB fold outward as would the outward V-fold $OACB$. Then path ACB remains entirely inside wedge W_i throughout the motion, and therefore does not interact with portions of P in different wedges. Furthermore, by Theorem 5, the various boundary portions in wedge W_i do not touch each other throughout the motion. It follows that this is indeed a continuous planar motion of L_1. □

The rest of the construction shows how to add additional support to L_1 to turn it into a one-degree-of-freedom linkage whose motion has the form described in the proof of Lemma 3. We cut down the freedoms of L_1 in several steps, given in the next three subsections.

4.3 Constraining Wall Segments to Rotations

For two non-overlapping segments PQ and RS whose lines intersect at a point O, consider the *rotation gadget* as illustrated in Figure 13. (When we apply this below, PQ and RS will be wall segments, and O will indeed be the crease point.) This linkage is specified as follows: $AB \parallel DE$ are any two segments not sharing an endpoint with PQ or RS with AB closer to O than DE; C is chosen on AB such that $OA+AC = OB+BC$, and the 180° angle at C is declared to fold outward, with F on DE chosen similarly; G is chosen so that $DACG$ is a parallelogram, and likewise $CBEH$ is a parallelogram.

Lemma 4. *The linkage illustrated in Figure 13(a) has one degree of freedom. If PQ and point O are held fixed in the plane, then in the unique motion, segment RS rotates rigidly around point O from its starting position to a closed configuration where PQ and RS are collinear.*

Proof. First note that, in this original configuration, O, C, and F are collinear by similarity of triangles AOB and DOE. By similarity of $\triangle AOB$ and $\triangle GCH$, it follows that the side lengths of quadrilateral $CGFH$ are proportional to those of $OACB$ and $ODFE$, and in particular, $CG+GF = CH + HF$,

To see that the linkage has one degree of freedom, note that if the shape of any one of parallelogram $ACGD$, parallelogram $CBEH$, or V-fold $CGFH$ is known, then all three are uniquely determined.

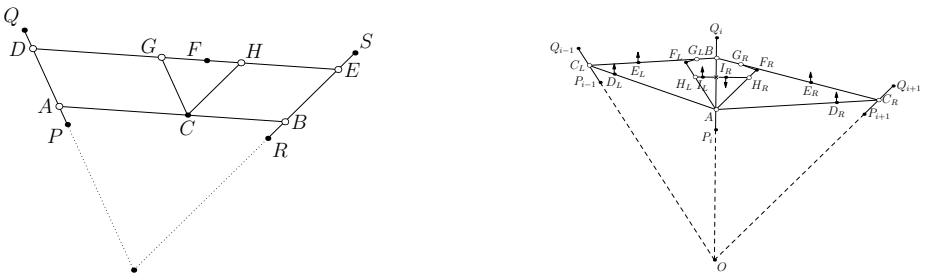

(a) The rotation gadget

(b) The synchronizing gadget

Figure 13: The two gadgets analyzed in Lemmas 4 and 7

To verify that this motion has RS rotating rigidly around O, suppose we have any other configuration of the linkage where vertex B has moved to B', C has moved to C', and so on, where A, D, P, Q, O have not moved but line RS is not known to pass through O. Let $O' = PQ \cap R'S'$. Because the lines of quadrilateral $C'G'F'H'$ are parallel to the corresponding lines of $O'DF'E'$, and we know that $DF'/F'E' = G'F'/F'H'$, it follows that quadrilaterals $O'DF'E'$ and $C'G'F'H'$ are similar. Because $OD/DF = CG/GF = C'G'/G'F' = O'D/DF'$, it follows that $OD = O'D$, so $O = O'$. Similarly, this proportionality gives $OE = OE'$, so RS has indeed simply rotated about O. This also implies that the linkage stays planar during the folding motion. □

Lemma 5. *Let L_2 be the linkage derived from L_1 as follows: for every internal cell, attach a rotator gadget inside the cell connecting (internal subintervals of) the wall segments. Then the motions of L_2 correspond exactly to those motions of L_1 where wall segments only rotate around O, and planar motions of L_1 extend (uniquely) to planar motions of L_2.*

Proof. In one direction, we must show that any configuration of L_2 has the property that every wall segment only rotates about O. Because any wall segment on ray r_1 clearly is constrained to rotating about O, the result follows from Lemma 4 paired with the fact that P is simple and hence the graph of cell adjacency is connected.

In the other direction, we must show that any non-overlapping planar motion of L_1 induces a non-overlapping motion of L_2. Specifically, we must show that the rotation gadgets do not introduce crossings. But this follows from Theorem 5, because the flat, outward V-folds composing the rotation gadget (ACB and DFE in Figure 13) are initially inside their cell (which in turn is bounded by flat, outward V-folds) and thus do not overlap during the motion. □

4.4 Synchronizing Wall Segments

We next show how to synchronize the wall segments to ensure that all wall segments originally on ray r_i remain on a single ray through O throughout any continuous motion. Let $\phi_1, \ldots, \phi_{t-1}$ be the initial angles of the wedges $W_1, \ldots, W_{t-1}$. For an internal cell $ABCD$ with $AB \subset r_i$ and $CD \subset r_{i+1}$, we know that any motion of L_2 rotates AB and CD around O, and we define the *angle* of the cell at any time as the angle between rays OAB and OCD.

Definition 2. *For each $1 \le i \le t-2$, construct a linkage M_i with two adjacent flat V-folds as follows. Points A, D, B, E, C are collinear, and connected in order (with B a flap on bar DE), and point O connects to A, B, and C. Angle OBA is $90°$, $\angle AOB = \phi_i$, and $\angle BOC = \phi_{i+1}$. Finally,*

if i is even then $OADB$ is an outward *flat V-fold and $OBEC$ is an* inward *flat V-fold, and if i is odd then $OADB$ is chosen outward and $OBEC$ is inward.*

Lemma 6. *The linkage M_i defined as above has a single degree of freedom and folds from the initial configuration to a flat one without overlap. Furthermore, there is a continuous, strictly increasing, and invertible function $m_i : [0, \phi_i] \to [0, \phi_{i+1}]$ such that $m_i(\angle AOB) = \angle BOC$ during this motion.*

Proof. Each V-fold is a one-degree-of-freedom mechanism and they are linked by the flap at B, so M_i has one degree of freedom. The existence of a continuous and strictly increasing function m_i follows from the fact that as M_i folds toward its flat state, all angles between bars increase or decrease strictly. These imply that m_i has a continuous and strictly increasing inverse. □

Inductively define $\Phi_1(s) = s$ and $\Phi_i(s) = m_{i-1}(\Phi_{i-1}(s))$; these will control the rates at which internal cells' angles change. Specifically, fix an internal cell $X_1Y_1Y_2X_2$ with two wall segments X_1Y_1 and X_2Y_2 such that $X_1Y_1 \subset r_1$ and $X_2Y_2 \subset r_2$ initially. (We may have $X_1 = X_2 = O$.) Let s be a variable representing the angle of cell $X_1Y_1Y_2X_2$ during any motion. We will brace L_2 to a new linkage so that every internal cell initially in W_i will have angle $\Phi_i(s)$ during the motion.

To do this, we make the following additions to L_2 to form a new linkage L_3: For every pair of adjacent internal cells with wall segments $P_{i-1}Q_{i-1} \subset r_{i-1}$, $P_iQ_i \subset r_i$, and $P_{i+1}Q_{i+1} \subset r_{i+1}$ (note that P_iQ_i need not be the maximal wall segment for either cell), attach a *synchronizing gadget* as shown in Figure 13(b)and described in detail below. Specifically, make the following additions to L_2 to form a new linkage L_3: For every pair of adjacent internal cells with wall segments $P_{i-1}Q_{i-1} \subset r_{i-1}$, $P_iQ_i \subset r_i$, and $P_{i+1}Q_{i+1} \subset r_{i+1}$ (note that P_iQ_i need not be the maximal wall segment for either cell), attach bars as shown in Figure 13(b). Specifically, AB is some subsegment of P_iQ_i not containing any vertices of P_iQ_i, and C_L and C_R are points of $P_{i-1}Q_{i-1}$ and $P_{i+1}Q_{i+1}$, and these are chosen so that triangles ABC_L and ABC_R do not intersect any rotation gadgets of L_2. Points D_L, E_L, D_R, E_R form outward V-folds as shown, and quadrilaterals AF_LG_LB and AF_RG_RB are drawn similar to quadrilaterals OC_LE_LB and OC_RE_RB. Finally, a segment H_LH_R is drawn perpendicular to AB with $H_L \in AF_L$ and $H_R \in AF_R$ (this is possible because $\phi_{i-1}, \phi_i < 90°$), with a sliceform at J. Finally, an outward (resp. inward) V-fold is drawn at I_L if i is even (resp. odd), with an inward (resp. outward) V-fold at I_R. The resulting construction is called a *synchronizing gadget.*

Lemma 7. *Define L_3 as the linkage constructed from L_2 by inserting a synchronizing gadget between every pair of adjacent internal cells as described above. Then the continuous motions of L_3 correspond to those motions of L_2 such that the angle of any internal cell originally in wedge W_i is now $\Phi_i(s)$, where s represents the (changing) angle of cell $X_1Y_1Y_2X_2$. Furthermore, planar motions of L_2 induce planar motions of L_3.*

Proof. Recall that all motions of L_2 can only rotate the wall segments about O. The synchronizing gadget is constructed to ensure that, during any motion of L_3, quadrilaterals OC_LE_LB remains similar to AF_LG_LB throughout the motion, and in particular, $\angle C_LOB = \angle F_LAB$ throughout. Similarly, $\angle BOC_R = \angle BAF_R$ throughout the motion. And because $AH_LI_LJI_RH_R$ forms a copy of linkage M_{i-1}, it follows that $\angle BOC_R = \angle OAF_R = m_{i-1}(\angle F_LAB) = m_{i-1}(\angle C_LOB)$. The claim that the angle of each cell originally in each wedge W_j is $\Phi_j(s)$ (where s is as in the theorem) now follows by induction on the length of the shortest path from each cell to cell $X_1Y_1Y_2X_2$.

We must also ensure that all such motions of L_2 extend to planar motions of L_3. Each internal cell now has a rotation gadget and possibly many parts of syncronizing gadgets, but each of these

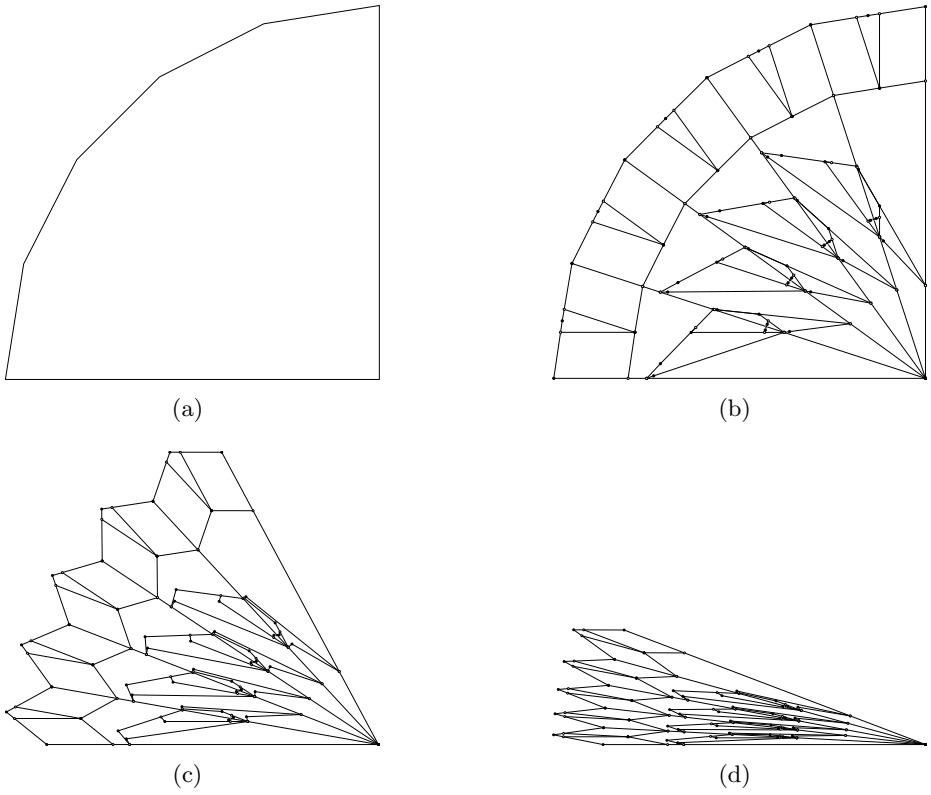

Figure 14: Applying the Pop-up algorithm from Theorem 6 to a fan-shaped polygon.

is bounded by flat outward V-folds, so they do not intersect each other by Theorem 5. The only potential intersection *within* a synchronizing gadget is that F_L may intersect segment AD_L, and similarly on the other side. It can be shown from Lemma 2 that rays AD_L and OC_L always intersect, and because AF_L remains parallel to OC_L, it follows that angle F_LAD_L never shrinks to 0 unless $P_{i-1}Q_{i-1}$ and P_iQ_i become collinear. □

4.5 Constraining Ear Cells

The configurations of all internal cells in L_3 are determined by $s = \angle Y_1OY_2$. The only unwanted degrees of freedom of L_3 must therefore come from the ear cells, which have not yet been modified. In this section we constrain these to produce the final linkage L.

Consider an ear cell with wall segment $P_iQ_i \in r_i$ and wall point $V_{i+1} \in r_{i+1}$, say. This is adjacent to a unique interior cell, with wall segment $P_{i-1}Q_{i-1}$ along r_{i-1}. To constrain ear cell $P_iQ_iP_{i+1}$, we simply add *two* synchronization gadgets centered on P_iQ_i that both connect to $V_{i+1} \in r_{i+1}$ and some point $V_{i-1} \in P_{i-1}Q_{i-1}$. Adding these synchronization gadgets for each ear cell produces the final linkage L:

Theorem 6. *The linkage L obtained from L_3 by adding two synchronization gadgets to each ear cell is a pop-up for the polygon P. Its boundary is connected and forms the polygon P in its opened configuration, and there are $O(n^2)$ total bars in the linkage.*

Proof. Consider the motion of L_3, parametrized by $s = \angle Y_1OY_2$, that rotates V_{i+1} so that $\angle Q_iOV_{i+1} = \Phi_{i+1}(s)$, and similarly for all other ear cells. This describes a continuous, planar motion of L_3 (of the form described in Lemma 3), and it follows from the analysis in the previous section that this extends to a continuous, planar motion of L.

We must show that L is a one-degree-of-freedom mechanism. We will show that s parameterizes the one degree of freedom, and as mentioned above, it suffices to show that the location of point V_{i+1} depends only on s. But this can be easily derived from properties of rotator gadgets.

The boundary of L is unchanged from that of P other than the insertion of vertices, so it is connected. Finally, there are $t = O(n)$ rays $r_1, \ldots, r_t$ which gives L_1 at most $O(n^2)$ bars, and each of the $O(n^2)$ rotator gadgets and synchronizing gadgets has $O(1)$ bars.

An example of this algorithm applied to a fan-shaped polygon is shown in Figure 14. □

5 Orthogonal Polyhedra Pop-Ups

In this section, we apply some of the techniques of 2D pop-up folds to the design of 3D pop-up structures that take the shape of orthogonal polyhedra. We first show how to construct pop-ups with an opening angle of 90°, then extend the construction to larger opening angles.

5.1 3D Pop-Up Model

In the 3D case, we model a pop-up using a model similar to *rigid origami*. A structure in rigid origami is composed of a number of infinitely thin rigid sheets of paper, each in the shape of a simple polygon, connected using hinged joints. If two sheets are joined at a hinge and one is held fixed, then the only possible motion for the other is rotation around the hinge. A hinge may also join more than two sheets, placing the same restriction on motion. A fold or a crease in a pop-up is equivalent to a hinge connecting two sheets. A flap in a pop-up corresponds to attaching the edge of one sheet to the center of another.

Let P be a simple polyhedron with n vertices $v_1, v_2, \ldots, v_n$. We select one edge e in P to be the *spine* of the pop-up. Let the faces adjacent to e be f_1 and f_2. The *opening angle* of the pop-up is the measure of the dihedral angle between f_1 and f_2. The *cover* of the pop-up consists of the union of two halfplanes. The first halfplane in the cover is the half of the supporting plane of f_1 that contains f_1 and has the extension of e as its boundary. The half of the cover containing f_2 is defined similarly.

A rigid-origami structure L is a *3D pop-up* for P if it has an open configuration, a closed configuration, and a unique folding motion from open to closed, all defined analogously to the configurations of a 2D pop-up. Specifically, the following conditions must hold:

(1) There exists a configuration of L such that the outer surface of the union of all of the sheets in L is equal to the boundary of P, and fhat e is in the same location as h. We call this the *open configuration.*

(2) There exists a configuration of L such that all sheets lie in the same plane, and all sheets lie on the same side of the line through h. We call this the *closed configuration.*

(3) There is a unique motion that transforms the open configuration into the closed configuration. During this motion, L is contained inside the wedge defined by the cover, and the opening

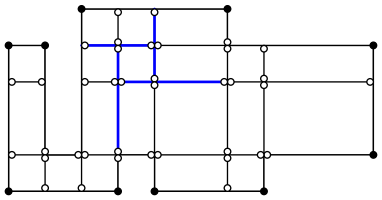

Figure 15: A pinwheel pattern. The rigid bars surrounding one cell are highlighted in blue.

angle decreases continuously. Just as in the 2D case, we assign all hinges in the pop-up structure a particular direction to fold in.

The *combinatorial complexity* of the 3D pop-up L is equal to the number of hinges.

Note that unlike in the 2D case, it is not sufficient to simply add more paper and more creases. By the Bellows Theorem [28, 9], if we treat a polyhedron as a linkage where each face is rigid and faces must rotate around edges, then all motions of the linkage preserve the volume of the polyhedron. Hence, we cannot fold the polyhedron flat unless we cut the boundary of the polyhedron.

5.2 Scaffold Pop-Ups

Suppose we have a simple orthogonal polyhedron P with an opening angle of 90°. Without loss of generality, we may assume that e lies along the z-axis, and that f_1 lies in the positive x section of the xz plane. Suppose further that f_2 lies in the positive y section of the yz plane. In our first step, we construct an orthogonal grid. Let $x_1, \ldots, x_n$ be the x-coordinates of all vertices in P sorted in increasing order. Similarly, let $y_1, \ldots, y_n$ be the sorted y-coordinates and let $z_1, \ldots, z_n$ be the sorted z-coordinates. Then *grid cell* (i, j, k) is the rectangular box $[x_i, x_{i+1}] \times [y_j, y_{j+1}] \times [z_k, z_{k+1}]$. By construction, the polyhedron P is the union of a face-connected subset R of grid cells. The *scaffold* of P is the union of all faces f of cells in R such that f is parallel to the spine.

The *grid slice* G_k consists of the union of all grid cells (i, j, k), not necessarily contained in P. Let the *slice scaffold* S_k be the intersection of the scaffold with G_k. The slice scaffold contains no faces perpendicular to the z-axis, and every cross section perpendicular to the z-axis is the same. Hence, the problem of constructing a pop-up for S_k is purely 2D.

To construct a pop-up for S_k, with the correct shear motion, we must find a way to combine faces of S_k into larger rigid sheets so the structure shears in the way we want. Say that we have an edge bordering exactly three faces. Then two of the faces must be coplanar, and can be merged into a single rigid sheet. The third face can be added as a flap to the middle of the larger sheet. Now say that we have an edge with x and y coordinates (x_i, y_j) bordering exactly four faces. Then there are two pairs of coplanar faces, which gives us two possible choices for the way to rigidify. If $(i + j)$ is even, then we rigidify the pair of faces perpendicular to the x-axis; otherwise, we rigidify the pair of faces perpendicular to the y-axis. This construction means that the four sheets adjacent to a given grid cell are arrayed in a pinwheel pattern, as depicted in Figure 15.

Suppose that we use this construction to make a pop-up-like structure for each slice, which we will call a *pinwheel slice*. Now suppose that we place them all side-by-side so that the initial position takes the shape of the scaffold. Call the result of this process the *sliced pinwheel scaffold*. Unfortunately, the sliced pinwheel scaffold is not a actually a pop-up for the scaffold: each slice scaffold is disconnected from its neighbors, and even within a single slice the slice scaffold may be

disconnected. To resolve this, we need a way to make the motions of one pinwheel slice affect the motions of its neighbors.

Given any pair $r_1, r_2 \in R$ of adjacent cells in adjacent slices, we wish to cause any motions of the sheets around r_1 to affect the sheets around r_2. For each such pair r_1, r_2, we fuse each of the four sheets that surround r_1 in the initial configuration with the corresponding coplanar sheet around r_2, to create four larger rigid sheets in the initial opening configuration. Call the result of this fusing the *pinwheel scaffold* of P.

Lemma 8. *The pinwheel scaffold of a polyhedron P is a pop-up for the scaffold of P. The pinwheel scaffold has complexity $O(n^3)$.*

Proof. By construction, the pinwheel scaffold has a valid open configuration, with the union of all sheets congruent to the scaffold of P. To see that it satisfies the other two properties of a 3D pop-up, we wish to show that if the opening angle α is given, then the location of each hinge is determined, and the mapping of hinges from their original locations is $f(x, y, z) = (x + y \sin\alpha, y \cos\alpha, z)$

We proceed by induction on the number of cells. Suppose that the locations for the hinges for the first ℓ cells satisfy the inductive hypothesis. Now consider a new cell $r_1 \in R$ that is face-adjacent to some cell $r_2 \in R$ in the set of ℓ cells. We consider two cases:

Case 1: r_1 and r_2 are in the same slice. By the construction of the pinwheel slices, if r_2 satisfies the shear mapping, then r_1 will also satisfy the shear mapping.

Case 2: r_1 and r_2 are in different slices. Then r_1 and r_2 share all four hinges, and so all of the hinges incident to r_1 must satisfy the shear mapping.

The complexity of the pinwheel scaffold is linear in the number of grid cell, for a total of $O(n^3)$. □

The pinwheel scaffold has a number of faces parallel to the spine. All such faces are contained within P when the scaffolding is open, and all faces on the boundary of P that are parallel to the spine also exist in the scaffolding (although they may be subdivided). The only missing pieces are the faces of P that are perpendicular to the spine.

5.3 Additional Faces

To add those pieces to the pinwheel scaffold, we first subdivide the faces using our rectilinear grid so that the sheets we wish to add to the pinwheel scaffold are faces of the grid cells. We must attach each such sheet to the sheets in the scaffold that form the adjacent grid cell.

There are four potential hinges that we could use to attach the new face to the scaffold. The two potential hinges we choose to use are the hinge parallel to the x-axis with the smallest y-coordinate, and the hinge parallel to the y-axis with the smallest x-coordinate. By construction, the angle between these two hinges will grow smaller as the pinwheel scaffold folds. Therefore, if we attach the new face using these hinges, we need not cut the resulting paper. Instead, it is sufficient to add a crease to the new sheet emanating from the intersection of the two hinges at a 45° angle. For consistency, we make each crease constructed in this fashion fold in the same direction (e.g. the positive z-direction). We call the resulting rigid origami structure the *draped scaffold*.

Theorem 7. *The draped scaffold of P is a pop-up for P with complexity $O(n^3)$.*

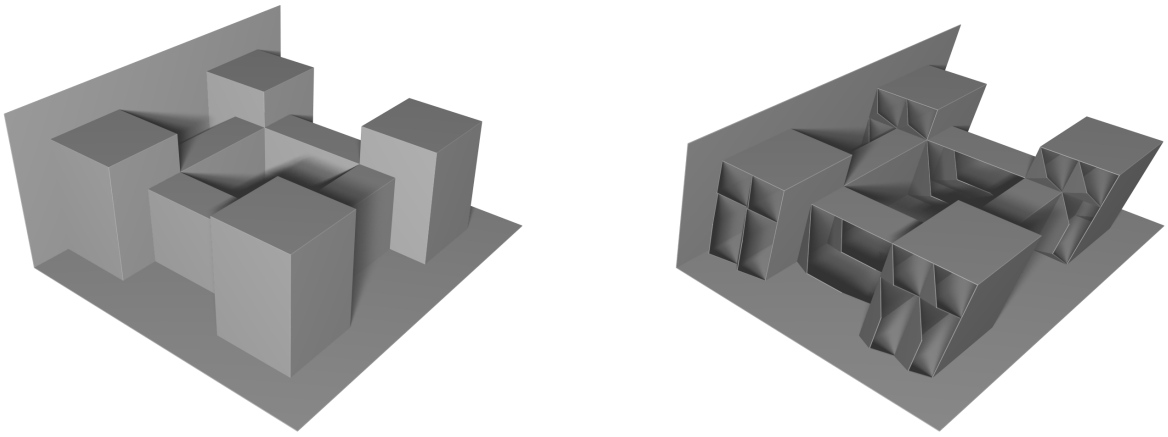

(a) The open configuration.

(b) An intermediate configuration

Figure 16: A 3D rendering of what the draped scaffold might look like for a particular 3D figure.

Proof. Just as in Lemma 8, our construction of the draped scaffold ensures that there exists an open configuration whose boundary is the target shape P. Furthermore, Lemma 8 shows that the pinwheel scaffold will uniquely fold into the closed state. Therefore, we need only consider how the new faces added to the pinwheel scaffold affect the way that it folds flat.

To show a unique folding motion, we first show that there is at most one way to fold the draped scaffold as the opening angle decreases. To see why, consider how a single added face will move as the opening angle decreases. The single face we add consists of two rigid sheets. Each rigid sheet shares a hinge with a sheet in the pinwheel scaffold, whose motion is entirely determined by the opening angle. As a result, the two newly added rigid sheets each have a single dimension of motion. The hinge joining the two sheets further restricts the motion of both, thereby ensuring that there is at most one way to place the newly added sheets, given the opening angle.

Next, we wish to show that the draped scaffold does fold — in other words, that there is at least one way to fold it as the opening angle decreases. To do so, we must check that folding the pop-up does not cause the sheets of the pop-up to self-intersect. Lemma 8 shows that no pair of sheets from the pinwheel scaffold can intersect each other. We must ensure that any sheets new to the draped scaffold will (a) not intersect with the pinwheel scaffold, and (b) not intersect with each other.

To show both these properties, it will be useful to consider the x- and y-coordinates of the new sheets during the fold. To that end, let points A through H be defined as in Figure 17, and consider what happens as $\angle ABC$ closes. The point E is equidistant from A and G when $\angle ABC = 90°$. Therefore, because sheets ABE and $BGCFE$ are rigid, E must be equidistant from A and G no matter what the measure of $\angle ABC$ is. So if we project the locations of each vertex onto the xy plane, E must lie on the angle bisector of $\angle ABC$. Furthermore, the distance between B and E is fixed, so in the xy projection it cannot get longer. This means that in the xy projection, E can

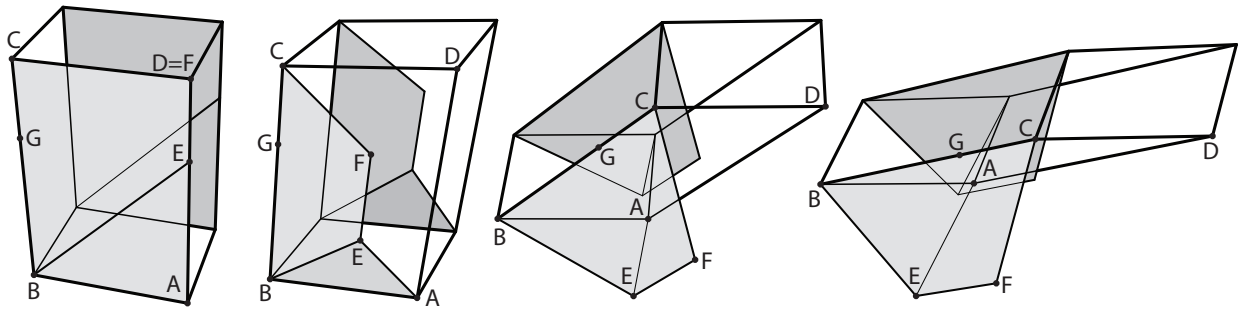

Figure 17: How to add faces perpendicular to the spine to the pinwheel scaffolding.

never leave the quadrilateral $ABCD$ even as the angle $\angle ABC$ shrinks.

How does the point G move in the xy projection of all points? The sheet $BGCFE$ is rigid, and hinged around the edge BC. As a result, if we consider BC to be held fixed, the only way for G to move is to rotate around the segment BC. Hence, in the xy projection, the x-coordinate of G will never change. Because the entire sheet $BGCFE$ is rigid, the y-coordinate of G will always be the same as the y-coordinate of E. As a result, G can never leave the quadrilateral $ABCD$ in the xy projection even as the angle $\angle ABC$ shrinks.

This shows that the new sheets added by the draped scaffold cannot intersect any of the sheets in the pinwheel scaffold. The only intersections that could potentially occur are between multiple draped scaffolds. Furthermore, this restriction on the x and y motion of new sheets means that the only way a pair of sheets can intersect is if the two sheets have the same x and y coordinates in the open configuration. But if the two sheets have the same x and y coordinates, then they will have exactly the same motion, translated by an amount equal to the initial z-distance between the sheets. As a result, there will be no intersections.

The complexity of the draped scaffold follows from the complexity of the pinwheel scaffold (from Lemma 8). The number of additional sheets added is no more than the number of grid cells, or $O(n^3)$. Hence, the total complexity is $O(n^3)$. □

Now that we know how to construct 90° pop-ups in 3D, we can extend our construction to handle larger multiples of 90° using a technique similar to the one in Section 3.2.

To modify our draped scaffold construction for opening angles of 180°, 270°, and 360°, it is possible to augment certain cells of the grid with a reflector gadget as we did for the 2D pop-up; however, the internal mechanisms of the reflector gadget might end up intersecting with the sheets used in the draped scaffold to simulate faces perpendicular to the spine.

Nonetheless, there is a way to solve this problem. First, we add four grid planes at coordinates $x = \pm\epsilon$ and $y = \pm\epsilon$, where ϵ is a constant strictly less than one third of the previous minimum distance between gridlines. This space around the axes is where we place our reflector gadgets. We choose the thickness (maximum difference in z-coordinates) of a single reflector gadget to be ϵ.

Suppose we embed a reflector gadget inside some pair of grid cells r_1, r_2. The grid cells r_1 and r_2 have thickness $> 3\epsilon$, while the reflector gadget has thickness ϵ. If the reflector gadget is centered, then the distance between the reflector gadget and any sheet that might get added to the draped scaffold is $> \epsilon$ when the pop-up is fully opened. The sheet added to the draped scaffold can protrude into the cell a distance of at most ϵ, because one of the dimensions of the cell is equal to ϵ. As a result, the sheet cannot intersect the reflector.

6 Conclusion and Open Problems

In this paper, we demonstrate techniques for designing 2D pop-ups for general polygons, and 3D pop-ups for orthogonal polyhedra. The most obvious open question is whether there is a way to construct 3D pop-ups for general polyhedra. Another question to consider is which 2D or 3D shapes are constructible using a single sheet of material with no gluing, as in most origamic architecture.

References

[1] Carol Barton. *The Pocket Paper Engineer: How to Make Pop-Ups Step-by-Step.* Popular Kinetics Press, Glen Echo, Maryland, 2005–2008. Two volumes.

[2] Marion Bataille. *ABC3D.* Roaring Brook Press, 2008.

[3] Duncan Birmingham. *Pop-Up Design and Paper Mechanics: How to Make Folding Paper Sculpture.* Guild of Master Craftsman Publications, 2010.

[4] David A. Carter. *One Red Dot: A Pop-up Book for Children of All Ages.* Little Simon, 2005. Other books include *Blue 2* (2006) and *600 Black Spots* (2007).

[5] David A. Carter and James Diaz. *The Elements of Pop-Up.* Little Simon, New York, 1999.

[6] David Cassell. Pop-up polyhedra. *Mathematics in School*, 17(1):24–27, January 1988.

[7] Masahiro Chatani. *Key to Origamic Architecture.* Shokokusha, 1985.

[8] Masahiro Chatani. *Pattern Sheets of Origamic Architecture.* Books Nippan, 1986. Two volumes.

[9] R. Connelly, I. Sabitov, and A. Walz. The bellows conjecture. *Beiträge Algebra Geom*, 38(1):1–10, 1997.

[10] John Lodge Cowley. *Solid Geometry.* London, 1752.

[11] Evermore Origamic Architecture. Pop-up card books. `http://www.evermore.com/oa/books.php3`, 2011.

[12] Andrew Glassner. Interactive pop-up card design, part 1. *IEEE Computer Graphics and Applications*, 22(1):79–86, 2002.

[13] Andrew Glassner. Interactive pop-up card design, part 2. *IEEE Computer Graphics and Applications*, 22(2):74–85, 2002.

[14] Takuya Hara and Kokichi Sugihara. Computer-aided design of pop-up books with two-dimensional v-fold structures. In *Abstracts from the 7th Japan Conference on Computational Geometry and Graphs*, Kanazawa, Japan, November 2009.

[15] Susan Hendrix. Popup workshop. `http://l3d.cs.colorado.edu/~ctg/projects/popups/`, 2007.

[16] Susan L. Hendrix and Michael A. Eisenberg. Computer-assisted pop-up design for children: computationally enriched paper engineering. *Advanced Technology for Learning*, 3(2), April 2006.

[17] Peter Hilton and Jean Pedersen. Constructing pop-up polyhedra. In *Build Your Own Polyhedra*, chapter 7, pages 101–105. Addison-Wesley, 1994. Based on an article "Pop-up Polyhedra" by Jean Pedersen, *California Mathematics*, April 1983, pages 37–41.

[18] Elliot E. Hui, Roger T. Howe, and M. Steven Rodgers. Single-step assembly of complex 3-D microstructures. In *Proceedings of the 13th Annual International Conference on Micro Electro Mechanical Systems*, pages 602–607, January 2000.

[19] Satoshi Iizuka, Yuki Endo, Jun Mitani, Yoshihiro Kanamori, and Yukio Fukui. An interactive design system for pop-up cards with a physical simulation. *The Visual Computer*, 27(6):605–612, 2011. Proceedings of Computer Graphics International 2011.

[20] Paul Jackson. *The Pop-Up Book: Step-by-Step Instructions for Creating Over 100 Original Paper Projects*. Holt Paperbacks, 1993.

[21] Scott Johnson and Hans Walser. Pop-up polyhedra. *The Mathematical Gazette*, 81(492):364–380, 1997.

[22] Xian-Ying Li, Chao-Hui Shen, Shi-Sheng Huang, Tao Ju, and Shi-Min Hu. Popup: Automatic paper architectures from 3D models. *ACM Transactions on Graphics*, 29(4):Article 111, 2010. Proceedings of SIGGRAPH 2010.

[23] Jun Mitani and Hiromasa Suzuki. Computer aided design for origamic architecture models with polygonal representation. In *Proceedings of Computer Graphics International*, pages 93–99, 2004.

[24] Jun Mitani, Hiromasa Suzuki, and Hiroshi Uno. Computer aided design for origamic architecture models with voxel data structure. *Transactions of Information Processing Society of Japan*, 44(5):1372–1379, 2003.

[25] Sosuke Okamura and Takeo Igarashi. An assistant interface to design and produce a pop-up card. *International Journal of Creative Interfaces and Computer Graphics*, 1(2):40–50, 2010.

[26] David Pelham. *Trail: Paper Poetry Pop-Up*. Little Simon, 2007.

[27] Ellen G. K. Rubin. A history of pop-up and movable books: 700 years of paper engineering. Public lecture, November 10 2010. `http://www.youtube.com/watch?v=iDJJOaZ1myM`.

[28] I. Kh. Sabitov. On the problem of the invariance of the volume of a deformable polyhedron. *Uspekhi Mat. Nauk*, 50(2(302)):223–224, 1995.

[29] Hugo Steinhaus. *Mathematical Snapshots*, pages 196–198. Oxford University Press, 1950. Republished by Dover Publications, 1999.

[30] Tama Software. Pop-up card designer. `http://www.tamasoft.co.jp/craft/popupcard_en/`, 2007. Pro version, `http://www.tamasoft.co.jp/craft/popupcard-pro_en/`, 2008.

[31] Ryuhei Uehara and Sachio Teramoto. The complexity of a pop-up book. In *Proceedings of the 18th Annual Canadian Conference on Computational Geometry*, Ontario, Canada, August 2006.

[32] Diego Uribe. *Fractal Cuts*. Tarquin, 1994.